中國機械工程學刊第四十卷第六期第 719~726 頁(民國一百零八年)
Journal of the Chinese Society of Mechanical Engineers, Vol.40, No.6, pp 719~726 (2019)

Tribological Behavior of Fe-32Mn-6Si Shape Memory Alloys

Amine Charfi *, Mohamed Trabelsi *, Tarak Bouraoui** and Mohamed Kharrat *

Keywords: Fe-based shape memory alloys, tribological behavior, microstructure.

ABSTRACT

Fe-Mn-Si based Shape Memory Alloys (SMA) present a good mechanical property with a low price compared with Ni-Ti and copper-based alloys, but the development of these alloys is limited to a few areas because of their low corrosion resistance. For this reason, an anticorrosion solution can be used to improve their resistance corrosion by the electrodeposition of a zinc layer followed by a trivalent chromate conversion layer.

Studies on wear behaviours in shape memory alloys are concentrated on Ni–Ti alloys but little studies are interested on Fe–Mn–Si alloys. To be used in industrial applications, the wear performances of shape memory alloys must be determined. This paper will present the wear properties of Fe-32Mn-6Si.

A comparison of the wear behaviour of Fe-32Mn-6Si at its different microstructural states: fully austenitic state (A1), duplex of austenite and thermal martensite state (A2) and finally a mixture of austenite and stress-induced martensite (A3) have been studied using reciprocating ball-on-flat tribometer. The effect of coating layer and the effect of lubrication on the tribological behavior of Fe-32Mn-6Si at its austenitic states were also studied.

The wear tests and the optical micrograph observations of the three microstructures show that the wear mechanism of shape memory alloys depended on the microstructure which was influenced by the amount of martensite presented in material. The wear behaviour of A1 and A2 is almost similar. Nevertheless, the wear resistance of A3 is the better due to the amount of martensite obtained by cooling is limited by the appearance of antiferromagnetism of the austenite structure during cooling. The results show also that the coating of material by an electrolytic zinc layer followed by a chromate conversion layer decreases its wear resistance that related to the formation of a zinc oxide layer that accentuates the wear mechanism. Wear test and optical micrograph show that lubricant improves the friction conditions of shape memory alloys.

Paper Received August, 2017. Revised August, 2018. Accepted October, 2018.Author for Correspondence: Amine Charfi.

* *University of Sfax, Laboratory of Electromechanical Systems (LASEM-ENIS), Sfax (Tunisia).*

** *University of Monastir, Mechanical Engineering Laboratory (LGM-ENIM), Monastir (Tunisia)*

INTRODUCTION

Fe-based shape memory alloys (SMA) have received considerable attention, since the single crystal of Fe–30Mn–1Si was discovered in the early 1980s (Sato et al., 1982; Sato et al., 1986), due to their low cost and high mechanical strength, as well as fine workability (Wan et al., 2005). Despite their distinctive properties, Fe–Mn–Si-based alloys are currently used in only a few practical applications such as tighteners or pipe couplings (Li et al., 2000) and civil engineering (Cladera et al., 2014). For these applications, the wear performance of material plays an important role to ensure its durability. For a better industrial development of these alloys, recent studies have focused on improving performance (Charfi et al., 2012), research for anti-corrosion solutions (Jemal et al., 2009) and numerical modeling of the thermomechanical behavior (Charfi et al., 2009).

The shape memory effect (SME) of these materials is governed by the stress-induced (fcc)$\gamma \rightarrow$(hcp)ε martensitic transformation and its reverse process upon heating. Various factors affect the martensitic transformation, among which the amount of pre-strain (Yang et al., 1992), annealing treatment (Mostafa et al., 2008, thermomechanical training (Chung et al., 1996; Xia et al., 1997; Lee et al., 2013) and alloy elements (Otsuka et al., 1990; Baruj et al., 2002; Peng et al., 2009; Tsuzaki et al., 1995). All these effects are highly correlated to the $\gamma \rightarrow \varepsilon$ martensite transformation which is a consequence of the reversible motion of the Shockley a/6<112> partial dislocation, as has been reported (Sato et al., 1982;

Sato et al., 1986). Studies on wear behaviour in SMAs are concentrated on Ni–Ti (Abedini et al., 2009; Ben Naceur et al., 2014) and Cu-based alloys, but little studies were carried out on Fe–Mn–Si alloys. Recent studies showed that wear resistance of Fe–14.51Mn–6.02Si–9.10Cr–5.06Ni–1.49Ti–0.16C alloy was much better than that of AISI 321 stainless steel and the wear resistance of material was remarkably improved by ageing with pre-deformation (Bu et al., 2011). Chengxin and al. (Chengxin et al., 2006) shows that the presence of a large amount of martensite in Fe–17Mn–5Si–10Cr–4Ni SMA in oily friction improves the wear resistance of alloy. In dry condition, the wear resistance of alloy is lower than that of 1Cr–18Ni–9Ti stainless steel.

The goal of this work was to study the tribological behavior of Fe-32Mn-6Si shape memory alloy at its different microstructural states: A1, A2 and A3 using reciprocating ball-on-flat tribometer testing to determine the influence of the microstructure on wear behavior of material.

This paper will present the effect of martensite structure on the wear resistance of Fe-32Mn-6Si alloy. The effects of thermal martensite state and the stress induced martensite state at room temperature have been investigated. The influence of lubrication and the coating of materials with an electrolytic zinc layer followed by a chromate conversion layer on wear resistance were also investigated.

EXPERIMENTAL PROCEDURE

Specimen preparation

Specimen of Fe-32Mn-6Si have been used in the present study is obtained from Aubert & Duval Company. The alloy was supplied as 18.18 mm² swaged bars and water quenched at a temperature of 1373 K. After this treatment, the specimens present a duplex structure of austenite and ε-martensite. The chemical composition of the alloy is given in Table 1. The 6.45 percent weight of Si is added in the aim to obtain an alloy with stacking fault energy which is proportional to the Gibbs free energy of the austenite-martensite transformation. Specimens have been cut (20 mm x 10 mm x 3 mm) by electro-erosion machining along the bar direction and then polished mechanically. The samples have been maintained at 873 K during one hour and then water cooled to room temperature. After this reference heat treatment, the alloy showed a fully austenitic structure at room temperature (Zhu et al., 1997; Bouraoui et al., 1996). The thermal martensitic structure of the alloy has been obtained by immersion of the alloy in liquid nitrogen for 5 minutes. However, to get a stress-induced martensite state, the alloy has been prestrained in tension utile 5% of deformation.

To observe the state of the material after friction test, an optical microscope is used.

Table 1: Chemical composition of the studied alloy (in wt %).

Fe	Mn	Si	C
Bal.	31.6	6.45	0.018

To compare the wear resistance of non-coated material with alloy that is coated by electrolytic zinc layer, samples has been coated to improve the corrosion resistance of the material. The zinc coating used is an industrial acidic bath. This type of coating is used in a temperature between 20 and 40 °C. The obtained coat is brilliant and ductile. This acidic bath technique is recommended to low and high carbon, cemented, soaked and melting steels. The zinc coating thickness is fixed and controlled at 10µm.

Electrical resistivity measurements

Electrical resistivity measurement has been carried out to identify the transformation temperatures of the Fe-32Mn-Si alloy. The setup has been done using four conductive wires welded on the 60 x 7.5 x 0.5 mm³ specimens (Bouraoui et al., 1996). The distance between the inner conductive wires l_o is 3 cm. The increase of temperature has been obtained by an electrical resistance furnace until the temperature of 650 K. Cooling has been done using a liquid nitrogen vapor (until 100 K). The cooling and the heating rate of 10 K.min^{-1} have been monitored by a proportional–integral–derivative (PID) controller. The imposed electrical current was 1 A and the variations of the electrical resistivity of the sample have been done referring to a type J thermocouple connected to the specimen. The electrical resistivity ρ (µΩcm) is given by the following expression:

$$\rho = \frac{SxU}{l0(1+ \alpha x \Delta T)} \ , \qquad (1)$$

Where S is the cross section of the specimen (7.5x0.5 mm²), U is the measured potential between the inner wires, l_0 is the distance between the inner thermocouples (3 mm), α is the thermal expansion coefficient of the studied alloy and ΔT is the difference between the time-dependent temperature and the room temperature 298K.

Optical micrograph of alloy

"Figure 1'' reproduces optical micrographs of the cross section of the etched specimens at different microstructural states. Figure a, b, and c show respectively A1, A2 and A3.

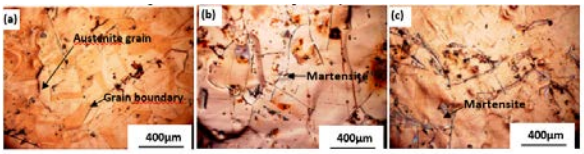

Figure.1: Optical micrographe of: (a) A1, (b) A2 and (c) A3

From figure 1.a, we notice that the microstructure of A1 presents a fully austenitic structure. “Figures 2.b and 2.c” show respectively a duplex structure of austenite and ε-martensite phases produced after cooling in liquid nitrogen for 5 minutes and by mechanical deformation at room temperature. The ε-martensite is localized around the grain boundary of the austenite parent phase. The rate of the ε-martensite phase obtained by heating is less important than the one produced mechanically. This result is also founded by electrical resistance measurements test of Fe-32Mn-6Si SMA which shows that during cooling, the forward transformation austenite-martensite failed at the appearance of the antifrromagnetism of the austenite phase.

Wear Test

The wear resistance of alloy at different microstructural states was performed using a reciprocating ball-on-flat tribometer (Fig. 2). The dimensions of the used specimens are 20 x 10 x 3 mm^3. The contact between the steel ball and the specimen is assured under a constant normal load. The material for the steel ball used in tribometer is 100Cr6 and the diameter of the ball is equal to 35 mm. As it shows in Fig. 2, the ball is set up and the sample below, the cyclic motion was applied to the specimen by using crank system driven by an electric motor with an electronic speed regulator. The tangential displacement amplitude and frequency were adjusted before the start of friction test. To measure the tangential force between ball and specimen, a load cell that is located between the specimen holder and the slider of the crank system allows is used. The output of this load cell was continuously stored by using a data acquisition system. The measurement frequency of friction coefficient is fixed and equal to 20 values per second.

Before each test, the steel ball and the sample surfaces were cleaned with ethanol. Each test is repeated at least three times to ensure the reproducibility of results. After each test, the surface morphologies of the wear tracks on the sample and on the steel ball were examined using optical microscope. The friction and wear test conditions used on our study are presented in Table 2

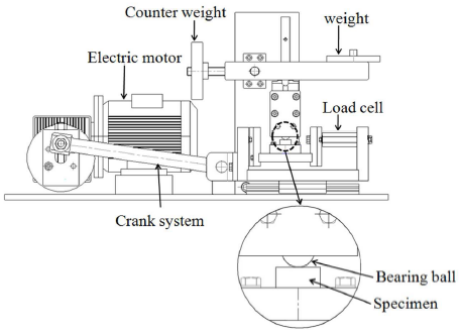

Figure. 2: Reciprocating ball-on-flat tribometer

Table 2: Parameters of tribological tests

Parameters	Values
Normal load (N)	81.3
Displacement amplitude (mm)	7.5
Frequency (Hz)	1
Temperature (°C)	20 - 25
Humidity (%)	50 - 60

After each wear test, we can measure the volume loss V and the wear rate K. The cross-section S (mm^2) of the wear groove on the sample surface was measured by established surface profile using SJ-210 Hand-held Roughness Tester. The volume loss V (mm^3) of the steel specimen due to the wear was calculated as: V = S.d.

Where d represent the length of the sliding stroke and equal to 15 mm.

The specific wear rate K (mm^3/Nm) was calculated using the following expression

$$K = V / (F_n x L), \quad \textbf{(2)}$$

Where Fn the normal load and L the sliding distance.

RESPONSE RESULTS AND DISCUSSIONS

Electrical resistance measurements

The transformation temperatures of Fe-32Mn-6Si are determined by electrical resistance measurements (Bouraoui et al., 1996). From this test we can determine the reverse transformation start temperature A_s, the reverse transformation finish temperature A_f, the antiferromagnetic transition temperature (T^{γ}_N the Néel temperature of the austenitic phase), the antiferromagnetic transition temperature T^{ε}_N (the Néel temperature of the martensitic phase) and the martensite starting temperature M_s of the alloy. The transformation temperatures are listed in table 3.

Table 3: Transformation temperatures of Fe-32Mn-6Si shape memory alloy (Bouraoui et al., 1996)

Ms ±5K	Mf ±5K	As ±5K	Af ±5K	T_N^{γ} ± 5K	T_N^{ε}± 5K
270	215	385	395	265	173

Hardness Test

The results of hardness measurements made on A1, A2 and A3 samples are shown in the following table

Table 4: Hardness values of A1, A2 and A3

	A1	A2	A3
Hardness (±5HV)	180	190	250

From table 4, we notice that the presence of a martensitic phase increases the hardness of materials. The average value of hardness for A1 and A2 that composed by a mixture of austenite and a few quantities of martensite is about 185HV. For A3 specimens that contain more quantity of martensite have an average value of hardness equal to 250HV. The alloys hardness increases with the amount of martensite in material.

Friction and wear properties

- **Friction behaviours**

"Figure 3" shows the typical evolution of the friction coefficients of Fe-32Mn-6Si shape memory alloy at different microstructure states (A1, A2 and A3) with the cycle number under the load of 81.3N. As shown in the figure, for the three samples, in the first stage it can be seen that the friction coefficients increase with the cycle number until reaching about 40000 cycles. After this value, the friction coefficients are almost constant until the end of the test. We notice so that the three samples have the same friction behavior. The friction coefficient of A3 is equal to 0.45 about that is higher than the two other samples (A1 and A2). The average value of the friction coefficient for these two samples is about 0.3.

The friction coefficient of shape memory alloy depends on different factors related to the quantity of different phases presented in material. However, A3 sample that contain the highest quantity of martensite has a significantly higher friction coefficient than the two other samples.

- **Wear behaviors**

"Figure 4" shows the typical profiles of the wear groove on Fe-32Mn-6Si shape memory alloy for A1, A2 and A3 using the Hand-held Roughness Tester after 80000 cycles of dry sliding.

From this figure we deduce that the three samples are worn with different degrees. A1 is the most worn sample and A3 is the less worn sample. This result is related to the difference of hardness value between A1 and A3.

From the typical profile of the wear groove for A1, A2 and A3 the cross section S of the wear grooves were calculated to determine the volume loss and draw plots that present the variation of volume loss against the cycle number and thereafter the specific wear rate K against the number of cycle. "Figure 5" represents the variation of volume loss against the cycle numbers for the three specimens (A1, A2 and A3).

Figure 5 shows the variation of volume loss of Fe-32Mn-6Si shape memory alloy at different microstructure states against the cycle number. It can be seen, for the three microstructures studied, the presence of two stages. The first is noted from the beginning of the test to 30000 cycles about which has a curved shape, after this value we notice a second stage where the variation of the volume loss is linear increases with the cycle number until the end of the test. We notice that the weight loss rate of A1 is more than that of A2 and A3, namely showing its poor wear resistance.

So a higher quantity of martensite presented in material increase its hardness and decreases the weight loss of material. Subsequently a higher amount of martensite improves the wear behavior of Fe based shape memory alloy (Chengxin et al., 2006).

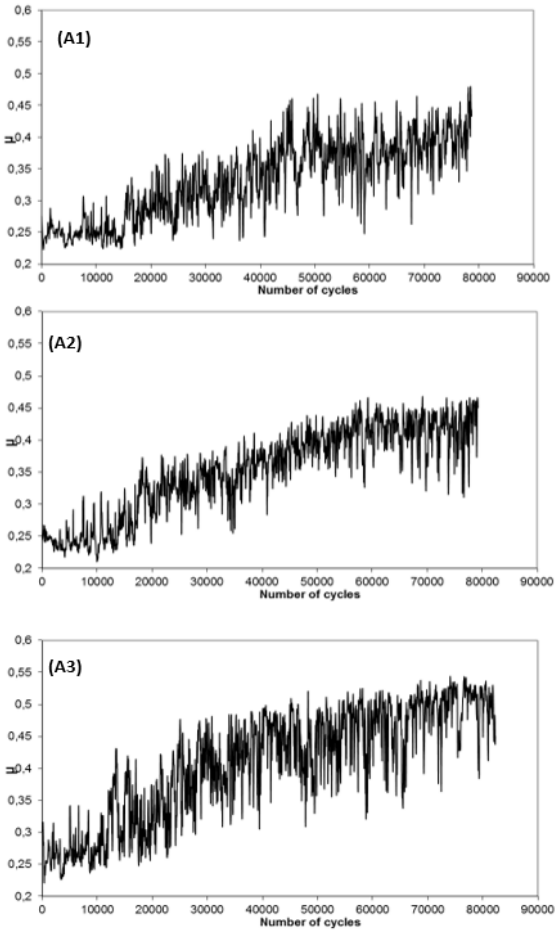

Figure. 3: Variation of friction coefficient against the cycle number under a load of 81.3 N

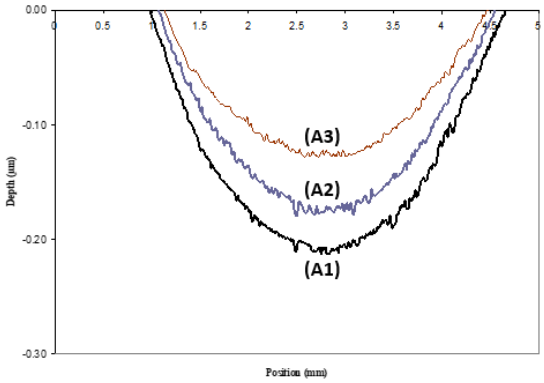

Figure. 4: Typical profiles of the wear groove

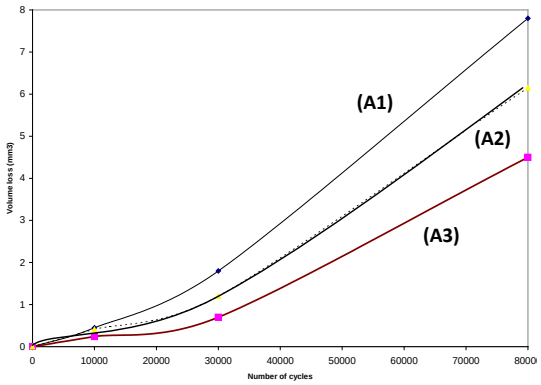

Figure. 5: Evolution of the volume loss against the cycle number

"Figure 6" shows the wear rate of A1, A2 and A3 as a function of cycle number. The figure shows an increase in wear rate of the material with increasing the cycle number. Therefore, the wear resistance of shape memory alloy degrades almost linearly when the number of cycles increases. A structure composed by austenite and stress induced martensite (A3) showed better wear resistance than the two other samples (A1 and A2).

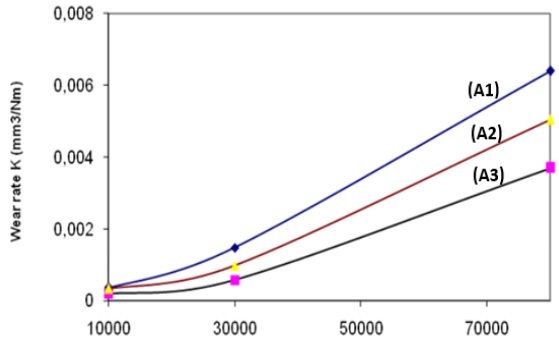

Figure. 6: Evolution of the wear rate against the cycle numbers

From figure 3 that present the variation of friction coefficient against the cycle number, we notice that the limit of the first stage is about 10000 cycles. To analyze the worn surfaces of the three specimens after 10000 cycles, a micrographic analysis was performed as is shown in "figure 7." From this figure we notice that the worn surface of A3 sample was relatively smooth, without the presence of groove. The high Vickers microhardness of this microstructure state explains this result (Lemma et al., 2015). For the two other samples, after 10000 cycles, we have almost the same wear state of the worn surface.

After 30000 cycles of wear and from "figure 8", we notice also a similar wear state for A1 and A2 and there are more wear grooves than that observed after 10000 cycles for A1 and A2. The A3 specimen presents the less wear grooves for the three specimens after 30000 cycles.

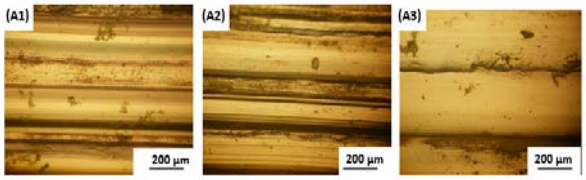

Figure. 7: Optical micrographs of the worn surface after 10000 cycles

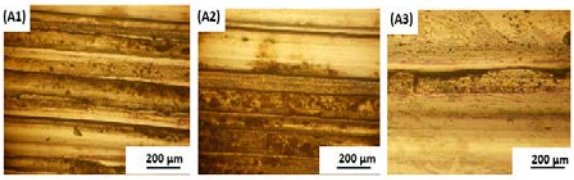

Figure. 8: Optical micrographs of the worn surface after 30000 cycles

"Figure 9" shows the optical micrographs of the worn surface of Fe–32Mn–6Si SMA specimens at its different microstructure states after 80000 cycles. It can be seen the presence of deeper wear traces on the surface of A1 and A2 specimens more than that presented in A3 specimen. The abrasion marks were parallel to the sliding direction. The A3 sample, which has the highest hardness value, was relatively smooth, with minimum of grooves. This superior wear resistance for A3 that is confirmed by previous tests is obtained from its microstructure that composed by an important quantity of martensite. The presence of this martensite state increases the wear resistance of material (Chengxin et al., 2006).

The presence of martensite phase in the shape memory alloy can play an important role in the friction and wear resistance. The martensite phase can affect the sliding wear by hardening the alloy.

From "figure 10", for A1, A2 and A3, an abrasive wear mechanism on the counter faces after 80000 cycles was observed. This mechanism was due to the effect of the hard debris formed during the wear test, the presence of steel particles and large fragments and the presence of a large pit on the surface of the ball. The wear of the ball in the case of A3 specimen is more important than for the two others. This result was attributed to the presence of a high amount of martensite in A3 specimen wich has a higher hardness compared with the austenitic phase.

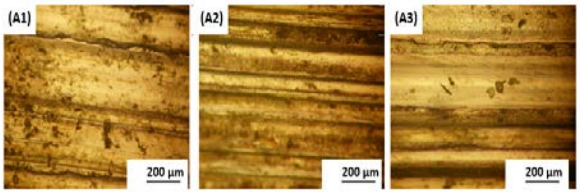

Figure. 9: Optical micrographs of the worn surface after 80000 cycles

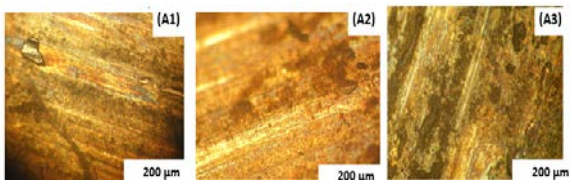

Figure. 10: Optical micrographs of balls after 80000 cycles

- **Effect of coating on wear behaviors**

"Figure 11" present the variation of friction coefficient against the cycle number for Fe-32Mn-6Si at its austenitic states (A1) coated by an electrolytic zinc layer and chromium conversion layer. This surface treatment improves remarkably the corrosion resistance of material without decrease the shape memory effect of material (Charfi et al., 2009). The results show that after 10000 cycles about, the friction coefficient is almost constant with an average value that equal to 0.5. Comparing this result with the non-coated sample at its austenitic structure (A1), we notice an increase of friction coefficient from 0.3 to 0.5. This increase of the friction coefficient is related to the presence of the zinc layer. This layer can be transformed to zinc oxide layer under the increase of temperature caused by the friction effect. The zinc oxide layer accentuates the wear mechanism.

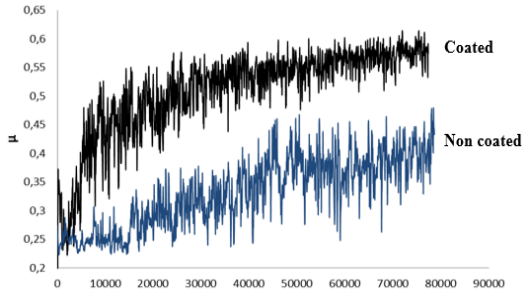

Figure. 11: Variation of friction coefficient against the cycle number for coated alloy

"Figure 12" present the micrographic analyze of specimen and ball after 80000 cycles. From figure we notice the presence of wear traces on the surface of alloy and a zinc layer bonded on the ball surface. The wear mechanism of the coating has been fatigued during the test and detached from the surface of shape memory alloy to be attached to the ball. With observing the micrographics photo, shows abrasive marks, pits and excess wear debris indicating that three body abrasive wear was the dominant wear mechanism.

- **Effect of lubrication on wear behaviors**

"Figure 13" present the variation of friction coefficient against the cycle number for A1 under lubrication. The lubricant used is the paraffin oil. We notice that under lubrication, the friction coefficient decrease from 0.3 under dry conditions to attain an average value of 0.18. Lubricant reduces the wear between the contact surfaces of shape memory alloy and the steel ball. Additionally, the paraffin oil provides a thin film between two contact surfaces that reduce wear and friction. This result is confirmed by micrographic photo

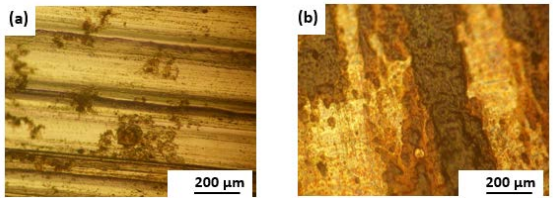

Figure. 12: Optical micrographs of worn surface (a) and ball (b) for coated alloy after 80000 cycles

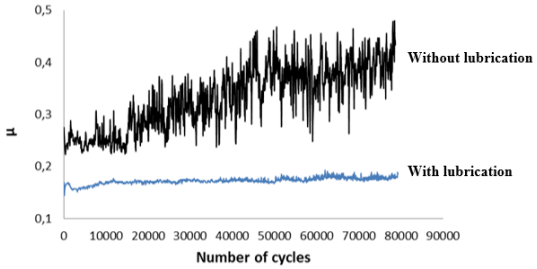

Figure. 13: Variation of friction coefficient against the cycle number for lubrication test

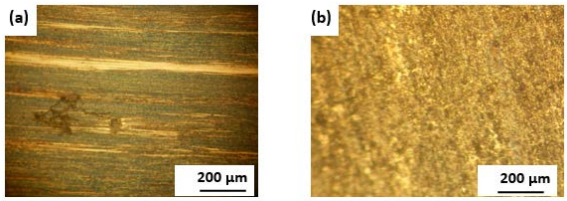

Fig. 14: Optical micrographs of worn surface (a) and ball (b) for lubrication test after 80000

From "figure 14" that present the micrographic analyze of sample and ball, we note a remarkable difference of the friction behavior between lubricated and non-lubricated material. After 80000 cycles, the wear traces are almost absent. We notice a partial regime of lubrication is predominant, both oil and boundary film play a role in wear mechanism. It was proven that paraffin oil is an excellent anti-wear and antifriction behavior.

CONCLUSIONS

The wear behaviour of Fe-32Mn-6Si SMA at its fully austenitic state (A1), mixture of austenite and thermal martensite (A2) and mixture of austenite and stress-induced martensite (A3) were investigated using a reciprocating ball-on-flat tribometer. The Tribological behavior of this nuance of SMA coated by an electrolytic zinc layer followed by a chromate conversion layer and the effect of lubricant were also studied. The wear behavior of single austenitic state (A1) is similar to the mixture of austenitic and thermal martensitic state (A2) that equal to 0.3 and presented a

friction coefficient lower than the mixture of austenite and stress-induced martensite (equal to 0.45). This behaviour is attributed to the fact that the amount of martensite obtained by cooling is limited by the appearance of antiferromagnetism of the austenite structure during cooling. A large amount of martensite in the shape memory alloy increases its hardness and improves its wear behaviour. The results show also that the coating of materials by an electrolytic zinc layer followed by a chromate conversion layer that increases the corrosion resistance of material and decreases its wear behaviors that attaint 0.5. This is due to the presence of third body debris composed by the zinc oxide layer under the increase of temperature. Finally it was concluded that lubricant improves the friction conditions of shape memory alloys. The average value of friction coefficient is equal to 0.18.

REFERENCES

Abedini, M., Ghasemi, H.M., and Nili Ahmadabadi M., "Tribological behavior of NiTi alloy in martensitic and austenitic states", Mater. & Design, 30, pp 4493-4497 (2009).

Ben Naceur I., Charfi A., Bouraoui T., Elleuch K., "Finite element modeling of superelastic Nickel-titanium orthodontic wires", J. Biomechanics, 47, pp 3630-3638 (2014).

Bu D., Peng H., Wen Y., Li N.; "Influence of ageing on wear resistance of an Fe–Mn–Si–Cr–Ni–Ti–C shape memory alloy", Mater. & Design, 32, pp 2969-2973 (2011).

Baruj A., Kikuchi T., kajiwara S., Shinya N.; "Effect of Pre-Deformation of Austenite on Shape Memory Properties in Fe-Mn-Si-based Alloys Containing Nb and C", Mater. Trans. JIM., 43, pp 585-588 (2002).

Bouraoui T., Tamarat K., and Dubois B., "Variations de résistivité électrique associées aux transformations martensitiques dans l'acier à mémoire de forme FM30", J. Phys. III, 6, pp831-841 (1996).

Chengxin L., Guixin W., Yandong W., Jingang W., Jianjun Z.; "Analysis of wear resistance and its mechanism in an Fe–Mn–Si–Cr–Ni shape memory alloy", Mater. Sci. & Engineering A, (438, pp 804–807 (2006).

Cladera A., Weber B., Leinenbach, C, Czaderski C., Shahverdi M., Motavalli M., "Iron-based shape memory alloys for civil engineering structures:An overview", *Constr. & Build. Mater.*, 63, pp 281 – 293 (2014).

Charfi A., Gamaoun F., Bouraoui T., Bradai C. and Normand B., "Shape memory effect improvement and study of the corrosion resistance of the Fe-8Mn-6Si-13Cr-6Ni-12Co alloy", *Adv. Mate. Rese.*, 476, pp 2162-2170 (2012).

Charfi A., Bouraoui T., Feki M., Bradai C. and Normand B., "Surface treatment and corrosion behaviour of Fe-32Mn-6Si shape memory allos", *C. R. Chimie*, 12, pp 270-275 (2009) .

Chung C.Y., Chen S. and Hsu T.Y., "Thermomechanical training behavior and its dynamic mechanical analysis in an Fe-Mn-Si shape memory alloy", *Mate. Charact.*, 37, N°4, pp 227-148 (1996).

Jemal F., Bouraoui T., Ben Zineb T., Patoor E. and Bradai C., "Modelling of Martensitic transformation and plastic slip effects on the thermo-mechanical behavior of Fe-based shape memory alloys", *Mech. Mater.*, 41, N°7, pp 849-856 (2009).

Lemma J.D., Warmuth A.R., Pearson S.R., Shipway P.H., "The influence of surface hardness on the fretting wear of steel pairs—Its role in debris retention in the contact", *Tribo. Inter.*, 81, pp 258–266 (2015)

Li J.C., and Jiang Q., "Shape memory effects in an Fe14Mn6-Si9Cr5Ni alloy for joining pipe", *ISIJ Int.*, 40, N°11, pp 1124-1126 (2000).

Lee W.J., Weber B., Feltrin G., Czaderski C., Motavalli M., Leinenbach C., "Phase transformation behavior under uniaxial deformation of an Fe–Mn–Si–Cr–Ni–VC shape memory alloy", *Mater. Sci. & Engine. A*, N° 1, p 581 (2013).

Mostafa K.M., De Baerdemaeker J., Van Caenegem N., Segers D. and Houbaert Y., "Study of the effect of annealing on defects in Fe–Mn–Si–Cr–Ni–C alloy by slow positron beam", *App. Surf. Sci.*, 255, N°1, pp 145-148 (2008).

Otsuka H., Yamada H., Maruyama T., Tanahashi H., Matsuda S. and Murakami M., "Effects of Alloying Additions on Fe-Mn-Si Shape Memory Alloys", *ISIJ Int.*, 30, pp 674-679 (1990).

Peng H.B., Wen Y.H., Ye B.B. and Li N., "Influence of ageing after pre-deformation on shape memory effect in a FeMnSiCrNiC alloy with 13 wt.% Cr content", *Mate. Sci. & Engine. A*, 504, N°1, pp 36-39 (2009).

Sato A., Chishima E., Soma K. and. Mori T, "Shape memory effect in γ→ε transformation in Fe–30Mn–1Si alloy single crystals", *Acta Metall.*, 30, N°3, pp 1177-1183 (1982).

Sato A., Yamaji Y. and Mori T., "Physical properties controlling shape memory effect in Fe-Mn-Si alloys", *Acta Metall.*, 34, pp 287-294 (1986).

Tsuzaki K., Natsume Y., Tomota Y. and Maki T., "Effect of solution hardening on the shape memory effect of Fe-Mn based alloys", *Scripta Meta. Uurgica et Makdia*, 33, N°7, pp 1087-1092 (1995).

Wan J., Chen S., "Martensitic transformation and shape memory effect in Fe–Mn–Si based alloys", *Cur. Opin. in Sol. State & Mater. Sci.*, 9, N°6, pp 303-312 (2005).

Xia R.D., Liu G.W. and Liu T., "The effect of thermal training on prestrained Fe-30Mn-6Si-5Cr shape memory alloy", *Mater. Letters*, 32, N°2, pp 131-136 (1997).

Yang J.H., Chen H. and Wayman, H., "Development of Fe-based shape memory alloys associated with face-centered cubic-hexagonal close-packed martensitic transformations: Part I. shape memory

behavior", *Metall. & Mater. Trans. A*, 23A, pp 1431-1436 (1992).
Zhu X. and Zhang Y., "Effect of ε-martensite on the electrochemical corrosion behaviour of an Fe-Mn-Si shape memory alloy in aqueous solutions", *J. Mater. Sci. Letters*, 16, pp 1516-1517 (1997).